Journal of Mines, Metals and Fuels, *71(11): 2089-2094; 2023. DOI: 10.18311/jmmf/2023/36098*

Print ISSN : 0022-2755

Journal of Mines, Metals and Fuels

Contents available at: *www.informaticsjournals.com/index.php/jmmf*

Experimental Investigation on Fracture Toughness of Hydrogen Embrittled Cu-Al-Be Shape Memory Alloy

S. Prashantha

Department of Mechanical Engineering, Siddaganga Institute of Technology, Tumkur – 572103, Karnataka, India; sprashantha@sit.ac.in

Abstract

Copper based Shape Memory Alloys (SMAs) possess good Shape Memory Effect (SME) and Superelasticity and the alloys are prone to corrosion due to atmospheric conditions. The SMAs absorb hydrogen which results in hydrogen embrittlement which affects the SMAs characteristics. The fracture toughness of the hydrogen embrittled alloys were estimated for compositions of ternary Alloy-Beryllium (0.47 by weight %) under uniaxial tensile testing (Mode –I type). Strain energy release rate and Stress Intensity factors were determined. 0.47 wt. % of Be in the SMA has the higher fracture toughness and the stress Intensity factor is directly proportional and strain energy release rate is inversely proportional with the increase in Crack length.

Keywords: *Cu-Al-Be, Fracture Toughness, Hydrogen Embrittlement, KIC, Shape Memory Alloy, Shape Memory Effect*

1.0 Introduction

The compatibility of Shape Memory Alloys (SMAs) made them to be considered for wide applications. The usage of NiTinol in orthodontics for its superiority owes to recovery force once deformed due to Shape Memory behaviour. The wires and brackets made of SMAs are prone to embrittlement due to the storage of H_2. The alloys in the presence of electrolytes affects the SMAs and results in galvanic corrosion[1-3]. It is observed that the corrosion is due to the presence of flourides due to the usage of toothpaste and prophylactic agents [4,5]. It is noticed that some SMAs break after a few months of setting and the deformability of the wires are lost[6,7].

Some of the modelling and experimental results concentrated on thermomechanical deformation and micromechanical behaviour[8,9]. The failure due to the fracture is important consideration in designing of structures or components. Fracture toughness term is used to measure the resistance of material for crack or flaw extension[10,11]. It is measured by considering the Stress Intensity Factor (SIF) of the specimen (KIC). ASTM E399 testing method is considered to be one of the accurate method for testing KIC of material with known Pre cracking for Single Edge Notched Bend (SENB) or Compact Tension (CT) type specimens. So circumferential notched specimen was used and results are recorded for tests[12].

The investigations on the hydrogen embrittlement mechanisms on NiTi alloys for thermal and mechanical behaviour were found that the presence of hydrogen suppresses the phase transformation. The tensile behaviour of the alloys has reported the appearance of two parts of the plateau, the first part was non-charged zone and the second part was charged zone with a heightening in stress and there was a decrease in strain in the upper plateau13. The fracture in case of tensile deformation test before and during stress induced martensite also revealed the cause of fracture is due to hydrogen embrittlement[13-15].

**Author for correspondence*

1.1 Fracture Toughness (K_{ic} and G_{ic})

It is measure of resisting the ability for the persisting crack flaw or crack and is used to design safe structures. For fracture analysis, Strain Energy Release Rate (SERR) and Stress Intensity Factor (SIF) needs to be determined.

1.1.1 Stress Intensity Factor (SIF)

The fracture toughness is characterised by Linear Elastic Farcture Mechanics (LEFM). The magnitude of stress at crack tip in a specific mode for homogenous elastic material gives SIF is denoted by K_I. As per this approach, the stress state at the tip of crack defines the SIF. When subjected to tensile loading, the crack growth reaches a critical value (K_IC) which causes the components to fail and the value is the alternate measure of fracture toughness. For round bar with circumferential notch, the expression to find K_{IC} is

$$K_{IC} = \{(Pf/D(3/2)) [1.72 (D/d) - 1.27]\} \quad (1)$$

For $1.2 < (D/d) < 2.1$, P_f is the Fracture load Dis the Diameter of un-notched round bar and d is Diameter of V-notched round bar.

1.1.2 Complience Caliberation

This method states the crack extends when the energy is sufficient to overcome the resistance of the material. The driving force for mode-I is the strain energy release rate (G_I). The material compliance is measured by the critical value of the energy release rate (G_{IC})which is the fracture toughness of the material and is found by

$$G_{IC} = \{(Pf\,2\,/2B)\,(dC/da)\} \quad (2)$$

Pf is the Fracture load, B is the width of the crack front = 2(Da – a 2) 1/2, and (dC/da) is rate of change of compliance to the rate of change of crack length.

2.0 Materials and Experimental Method

Cu-Al-Be shape memory alloy wires prepared by ingot metallurgy route with Cu-88.03 Wt.%, 11.5 Wt.% Al and 0.45 Wt.% Be with specimen diameter 12 mm was considered for the study. The prepared wires were subjected to homogenization for 30 minutes at 600^{0}C and the transformation temperatures were measured by DSC. The charging of hydrogen to the wires was done by electrolytic charging by DC. The rods were placed in sodium sulphate 1.0 Wt.% solution as cathode, austenitic stainless steel is made as an anode. The schematic view of the set up is shown in Figure 1.

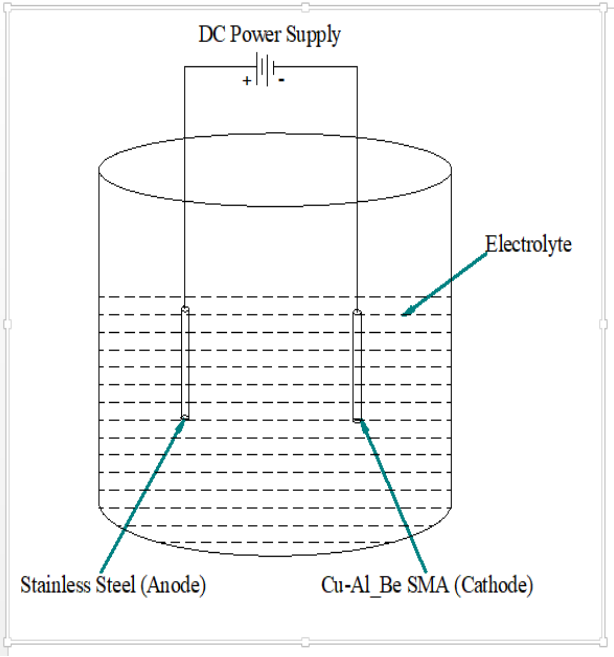

Figure 1. Schematic view of experimental set up for hydrogen charging.

The current density of 1000 A/m^2 was set up for the electrolytic charging process. Continuous monitoring of the electrical circuit was done by charging for 10 hours. The charged rods were subjected to aging studies for 10, 15 and 20 hours. The cracks were made in specimens with lengths of 1.25,1.75, 2.25 and 2.75 mm. Thus prepared specimens were subjected to testing to find the fracture toughness.

The equipment's in mining industry work under extreme moist to dry conditions, fracture due to hydrogen embrittlement is one of the major cause for failure of metals. This experiment methodology helps to understand the mechanism of metal/equipment fracture.

3.0 Results and Discussion

3.1 Composition and Transformation Temperature of the SMAs

The prepared samples were subjected to compositional analysis and DSC measurements to know the composition and transformation temperatures. The composition and

Table 1. Chemical composition and transformation temperature of SMA

Alloy ID	Chemical Compositions (in Wt. %)			Transformation temperatures in ^{0} C			
	Cu	Al	Be	M_f	Ms	As	A_f
CAB 1	88.03	11.5	0.47	42.3	57.2	67.6	86.6

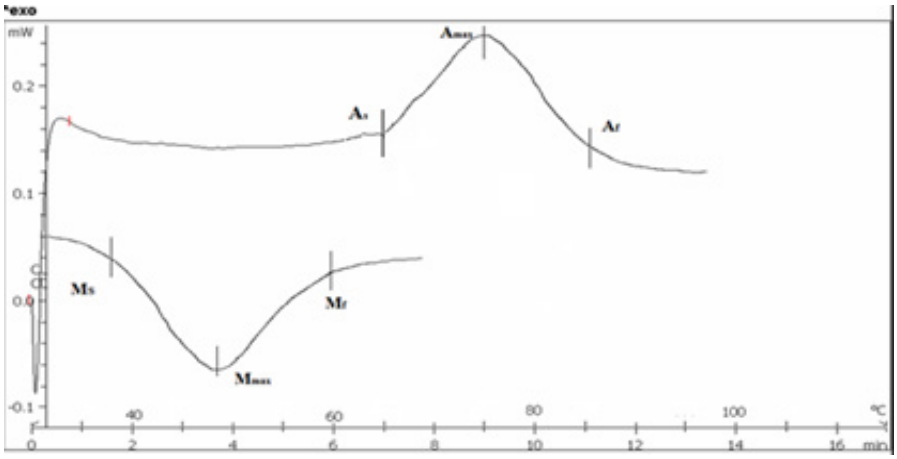

Figure 2. DSC plot of the SMA sample without charging and ageing.

transformation temperature of the prepared alloy are listed in Table 1.

Table 1 shows the composition and transformation temperature of the prepared alloy.

The DSC plot (Figure 2) for the alloy shows the transformation temperatures.

3.2 The Shape Memory Effect (SME)

The Shape Memory Effect (SME) of the alloy was calculated by bend test and SME obtained for a sample is 100% for the specimen without embrittlement. The SME for the charged and aged specimen shows the decrement in the SME may be due to the formation of precipitates with aging which changes the composition of the alloy thereby alters the SME. Table 2 shows the % of the change in SME.

The hydrogen embrittled pre cracked specimens were put for tensile testing to know the fracture toughness by K_{IC} and G_{IC} Mode-I condition. The specimen was charged and aged for 10,15 and 20 hours. There is more effect on transformation from austenite to martensite, which may be due to the absorption of H_2 and diffusion of H_2 in the CuAlBe matrix adds to the resistance to the transformation from martensite to Austenite.

Three different charged and aged specimens with crack length of 1.25,1.75, 2.25 and 2.75 mm were chosen and are subjected to uniaxial tensile loading up to fracture failure. The fracture load (P_f) at failure and the deflection

Table 2. Variation of Sme in % by Bend Test

Alloy	Before ageing	After10 hr.	After 15hr	After 20hr
CAB	99.8	96	84	62

(δ) were noted. The P_f indicates that as the length of the crack and load taking capacity are inversely proportional for all samples and the fracture toughness of Cu-Al-Be SMAs were found out by K_{IC} and G_{IC} data.

3.3 SIF approach

Figure 3 highlights the variation of K_{IC} for different crack lengths. The value of K_{IC} increases with increase in the crack length which may be due to the presence of Be in the alloy compared to other copper based alloys. The 20 hour aged sample shows higher value of K_{IC} compared to other aged specimens, it may be due to the presence of H_2 diffusion of H_2 into the core of the specimen.

The values of K_{IC} for different crack lengths, charged and aged specimens are represented in Table 3 and is calculated by

$$K_{IC} = \{(Pf/D(3/2)) [1.72 (D/d) - 1.27]\} \quad (1)$$

3.4 Compliance Calibration Method

Material stiffness is reciprocal of compliance and by knowing the stiffness, compliance can be found out. Figure 4 shows the variation in SERR (G_{IC}) of the alloys for different notch configurations. With increase in crack length, the G_{IC} value decreases and is calculated by

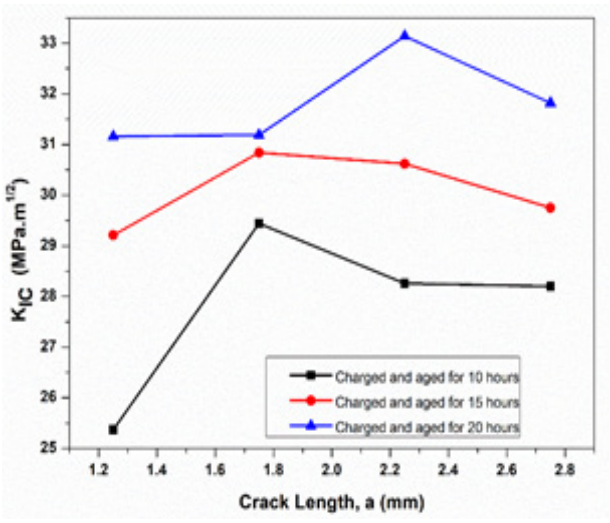

Figure 3. Variation of crack Length with KIC.

$G_{IC} = \{(Pf\ 2\ /2B)\ (dC/da)\}$. Table 4 shows the SERR for different crack lengths.

4.0 Conclusions

The SME of the specimen decreased from 100% to 62% for the charged and aged (20 hours) alloy and is due to

Table 3. Calculated K_{ic} values for different CNRB specimens

Specimen	Crack length 'a' in mm	(D/d) ratio	P_f in KN	K_{IC} in MPa√m
Charged and aged for 10 hours	1.25	1.2623	37.16	25.37
	1.75	1.4137	33.16	29.44
	2.25	1.6064	24.64	28.26
	2.75	1.8397	19.70	28.20
Charged and aged for 15 hours	1.25	1.2603	43.16	29.21
	1.75	1.4127	34.88	30.84
	2.25	1.5952	27.52	30.62
	2.75	1.8593	20.04	29.75
Charged and aged for 20 hours	1.25	1.2628	45.48	31.16
	1.75	1.4132	35.20	31.19
	2.25	1.5984	30.16	33.14
	2.75	1.8461	21.96	31.82

Table 4. Calculated G_{IC} values for different CNRB specimens

Specimen	Crack length 'a' in mm	'δ' in mm	Stiffness (Pf / δ) in KN/ mm	C = (δ/Pf) 10-3 (*mm*/kN)	Dc/da $(kN)^{-1}$	G_{IC} in MJ/m^2
Charged and aged for 10 hours	1.25	0.6	73.6	13.5869	0.0371	4.9326
	1.75	0.57	70.45	14.1932		3.5427
	2.25	1.07	29.57	33.8179		1.9927
	2.75	1.00	25.07	38.9105		1.2126
Charged and aged for 15 hours	1.25	0.57	85.01	11.7623	0.0342	5.8604
	1.75	0.53	79.02	12.6552		3.5525
	2.25	0.94	35.66	28.0429		2.0495
	2.75	1.17	22.25	44.9318		1.1584
Charged and aged for 20 hours	1.25	0.62	84.64	11.8140	0.040	7.5097
	1.75	1.01	41.78	23.9336		4.2109
	2.25	1.67	22.25	44.9408		2.9452
	2.75	1.52	19.05	52.4861		1.6628

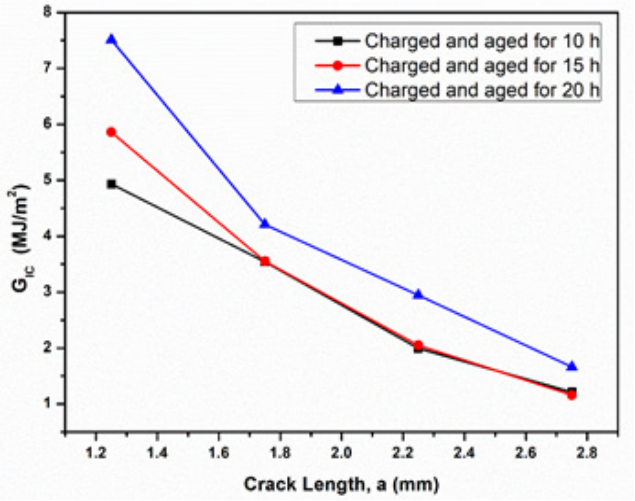

Figure 4. Variation of crack length with GIC.

the formation of precipitates with aging which changes the composition of the alloy The absorption of hydrogen in the specimen suppresses the phase transformation. Stress intensity factor (K_{IC} value) of the three samples increases with increase in crack length and it has also shown dependency on ageing in the alloy sample. Strain energy release rate (G_{IC} value) of the three charged and aged specimens decreases with increase in crack length. Hydrogen occupies the vacancies existing in between the copper and aluminium intermetallic bonds and as a result of this Stress intensity factor (K_{IC}) increases and of Strain energy release rate (G_{IC}) decreases.

Since the equipment's in mining industry work under extreme moist to dry conditions, fracture due to hydrogen embrittlement is major cause for failure of metals. This experiment methodology helps to understand the mechanism and outcomes help us to understand in better way and to mitigate the issues for long run of machines/ equipment's.

5.0 References

1. Asaoka K, Yokoyama K, Nagumo M. Hydrogen embrittlement of nickel-titanium alloy in biological environment. Metall Mater Trans A. 2002; 33(3):495-501. https://doi.org/10.1007/s11661-002-0111-8
2. Schiff N, Boinet M, Morgon L, Lissac M, Dalard F, Grosgogeat B. Galvanic corrosion between orthodontic wires and brackets in fluoride mouthwashes. Eur J Orthodont. 2006; 28:298-304. https://doi.org/10.1093/ejo/cji102 PMid:16428255

3. Prashantha S, Auradi V, Nagral M, Patil S. Effect of hydrogen embrittlement on the characteristics of copper-based shape memory alloy. Journal of Mines, Metals and Fuels; 2021:159-62. https://doi.org/10.18311/jmmf/2021/30148
4. Schiff N, Grosgogeat B, Lissac M, Dalard F. Influence of fluoride content and pH on the corrosion resistance of titanium and its alloys. Biomaterials. 2002; 23:1995-2002. https://doi.org/10.1016/S0142-9612(01)00328-3 PMid:11996041
5. Schiff N, Grosgogeat B, Lissac M, Dalard F. Influence of fluoridated mouthwashes on corrosion resistance of orthodontics wires. Biomaterials. 2004; 25:4535-42. https://doi.org/10.1016/j.biomaterials.2003.11.042 PMid:15120498
6. Harris EF, Newman SM, Nicholson JA. Nitinol arch wire in a simulated oral environment, changes in mechanical properties, Am J Orthod. 1988; 93508-513.
7. Hudgins JJ, Bagby MD, Erickson LC. The effect of long-term deflection on permanent deformation of nickel-titanium archwires. J Angle orthod. 1990; 60:283-88.
8. Miyazaki S, Otsuka K. Development of shape memory alloys. Journal de Physique. 1983; 29(5):353-77. https://doi.org/10.2355/isijinternational.29.353
9. Swamy MKR, Prashantha S, Mallikarjun US. Characterization of Cu-Al-Be shape memory alloys. IOSR Journal of Mechanical and Civil Engineering. 2012.
10. Dieter GE. Mechanical Metallurgy, SI edition. Singapore: McGraw-Hill; 1988. p. 348-68.
11. Ibrahim RN, Stark HL. Validity requirements for fracture toughness measurements from small circumferentially notched cylindrical specimens. Journal of Engineering Fracture Mechanics. 1987; 28(4):455-60. https://doi.org/10.1016/0013-7944(87)90190-1
12. Letaief WE, Hassine T, Gamaoun F. Tensile behaviour of superelastic NiTi alloys charged with hydrogen under applied strain. Materials Science and Technology. 2017; 33(13):1533-8. https://doi.org/10.1080/02670836.2017.1320084
13. Yokoyama K, Hamada K, Moriyama K, Asaoka K. Degradation and fracture of Ni-Ti superelastic wire in an oral cavity. Biomaterials. 2001; 22:2257-62. https://doi.org/10.1016/S0142-9612(00)00414-2 PMid:11456065
14. Gamaoun F, Hassine T, Bouraoui T. Strain rate response of a Ni-Ti shape memory alloy after hydrogen charging. Phil Mag Lett. 2014; 94(1):30-6. https://doi.org/10.1080/09500839.2013.855330
15. Gamaoun F, Ltaief M, Bouraoui T, Zineb. Effect of hydrogen on the tensile strength of aged Ni- Ti superelastic alloy. J Intel Mat Syst Str. 2011; 22(17):2053-9. https://doi.org/10.1177/1045389X11423427